PREDICTING FRAGMENTATION PROPAGATION PROBABILITIES FOR AMMUNITION STACKS

Dr. John Starkenberg, Ms. Kelly J. Benjamin, and Dr. Robert B. Frey
U.S. Army Research Laboratory, Aberdeen Proving Ground, MD

ABSTRACT

By combining several existing models, we have developed a tool for estimating probabilities associated with the propagation of detonation, burning, and mechanical damage between ammunition stacks. The models include the FRAGHAZ program for the Monte Carlo treatment of fragment trajectories and the accumulation of hit probabilities. The Jacobs-Roslund criterion for initiation of detonation, and a residual velocity condition for initiation of burning. We have applied this tool to stacks of artillery projectiles and missiles. Since the appropriate fragmentation input data was not always available, notably in the case of missiles, we developed methods of estimating this data. Single artillery projectile donors were shown to require a near-direct hit to initiate detonation in either artillery projectile or missile acceptor stacks. Artillery projectile donor stacks were shown to be much more lethal than missile donor stacks, and missile acceptor stacks were shown to be more vulnerable to the propagation of burning than artillery projectile acceptor stacks.

BACKGROUND

In conjunction with a study of the benefits of insensitive munition (IM) technology, a need arose to develop a methodology for prediction of the probabilities of propagation of reaction (detonation or burning) and mechanical damage between a detonating stack of ammunition and its neighbors as functions of the distance between them. Such a capability could provide input to further analyses to predict losses in a variety of combat scenarios.

An informal survey of propagation accident reports (summarized in Appendix A) indicates that the most common mechanism of reaction propagation involves ignition of fires (often in combustible packaging) by fragments, debris, or firebrands from the source explosion and subsequent violent reaction of munitions in those fires. The resulting chain of events may take hours or even days to unfold. This scenario appears to be too complex and variable to model at the present time.

In some other cases, fragments from the source (donor) explosion can promptly damage, ignite mild to violent burning in, or detonate the energetic components (not including any combustible packaging) of munitions in nearby (acceptor) stacks. When detonation results, reaction can propagate further by the same mechanism, rapidly consuming large quantities of ammunition. When only burning or mechanical damage results, the acceptor stack may be totally or partially destroyed, but no further propagation by the fragment mechanism ensues. This scenario is amenable to modeling.

In order to span the range of munition vulnerability, we wanted to obtain predictions applicable to typical (thick-walled) artillery projectiles and (thin-walled) missiles stacked on pallets. We also wanted to obtain predictions for a single artillery projectile donor representing an attacking munition which might be required to start the donor-acceptor chain in an analysis. We have chosen palletized and single M107 155-mm projectiles and palletized TOW-2A missiles as representative items.

Report Documentation Page

Form Approved
OMB No. 0704-0188

1. REPORT DATE	2. REPORT TYPE	3. DATES COVERED
AUG 1996		**00-00-1996 to 00-00-1996**

4. TITLE AND SUBTITLE	5a. CONTRACT NUMBER
Predicting Fragmentation Propagation Probabilities for Ammunition Stacks	5b. GRANT NUMBER
	5c. PROGRAM ELEMENT NUMBER
6. AUTHOR(S)	5d. PROJECT NUMBER
	5e. TASK NUMBER
	5f. WORK UNIT NUMBER
7. PERFORMING ORGANIZATION NAME(S) AND ADDRESS(ES) **U.S. Army Research Laboratory,AMSRL-WT-TB,Aberdeen Proving Ground,MD,21005-5066**	8. PERFORMING ORGANIZATION REPORT NUMBER
9. SPONSORING/MONITORING AGENCY NAME(S) AND ADDRESS(ES)	10. SPONSOR/MONITOR'S ACRONYM(S)
	11. SPONSOR/MONITOR'S REPORT NUMBER(S)

12. DISTRIBUTION/AVAILABILITY STATEMENT
Approved for public release; distribution unlimited

13. SUPPLEMENTARY NOTES
See also ADM000767. Proceedings of the Twenty-Seventh DoD Explosives Safety Seminar Held in Las Vegas, NV on 22-26 August 1996.

14. ABSTRACT
see report

15. SUBJECT TERMS

16. SECURITY CLASSIFICATION OF:			17. LIMITATION OF ABSTRACT	18. NUMBER OF PAGES	19a. NAME OF RESPONSIBLE PERSON
a. REPORT **unclassified**	b. ABSTRACT **unclassified**	c. THIS PAGE **unclassified**	**Same as Report (SAR)**	**30**	

APPROACH

We determined that the following elements are required to successfully model propagation among stacks of these items:

- Descriptions of the stack storage arrangements;
- Arena test data for donor stack munitions describing the initial fragment mass, velocity, and shape distributions, or estimates of such data;
- A treatment of fragment trajectories to determine hazard probabilities;
- Descriptions of the vulnerable components of the acceptor stack munitions; and
- Criteria for the initiation of detonation and burning as well as for mechanical damage.

The pallet arrangements commonly used for the weapons of interest have been determined. These form the building blocks for larger stacks.

Arena test data are generally available only for warheads whose performance is measured by fragmentation statistics. That is, data are available for the M107 projectile but not for the shaped-charge warhead and rocket motors found in the TOW-2A. We had to develop a method to estimate the data for the latter items.

We decided to modify an existing computer program called FRAGHAZ (McClesky 1988) in order to compute fragment trajectories and the desired probabilities. FRAGHAZ was developed to predict the hazard to a human target due to fragmentation from an exploding ammunition stack. Fragmentation data for a number of munitions are provided with the program.

Descriptions of the vulnerable components of these weapons were sometimes difficult to find. They were obtained from a variety of sources. In some cases, best guesses were used. In all cases, the geometries were represented as to simple cylindrical metal shells filled with energetic materials.

An initiation criterion for detonation is well known, and a simple criterion for burning may be developed from research data pertinent to this phenomenon

FRAGHAZ

FRAGHAZ uses a fourth-order Runge-Kutta scheme to compute trajectories for each fragment specified in the arena test input data. The trajectories include effects of ricochet and wind (if desired). All the fragments are assumed to emanate from a single vertical line extending from the base to the top of munitions in the face of the stack as shown in Figure 1. This defines the stack axis. The initial fragment height is selected at random within this range. The initial fragment velocity and elevation angle are selected at random in a range near the values given in the input data. Parameters used to determine the fragment drag coefficient are determined as functions of a randomly selected value. The program replicates these trajectory computations many times with randomly selected environmental conditions. While FRAGHAZ provides "Monte Carlo" and "Full Factorial" options, the random selections referred to in the foregoing description apply only to the Monte Carlo option.

A downrange "hazard volume," also shown in Figure 1, is defined. This consists of a cylindrical sector originating at the stack axis having a specified angular width (equivalent to the azimuthal sector associated with arena test data collection) and having the height of the target (nominally a 5.72-ft tall standing man). It is divided into a number of 100-ft annular segments. As each fragment passes through a hazard-volume

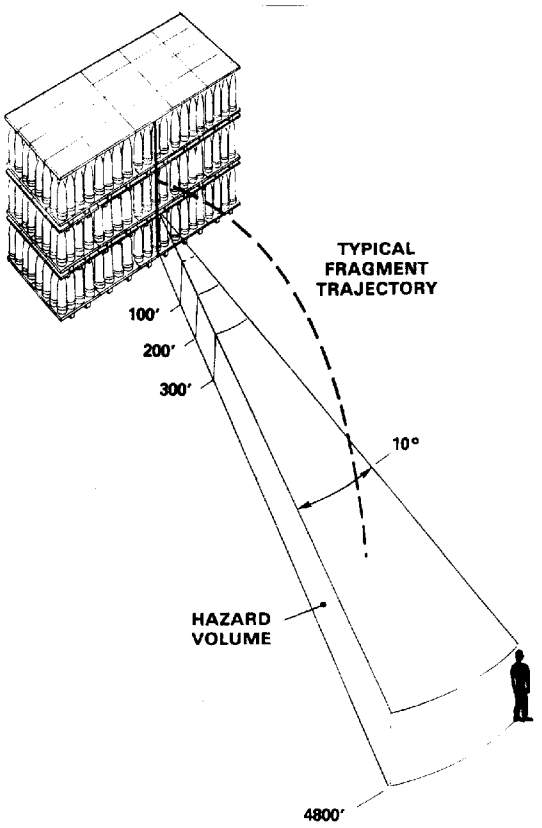

Figure 1. FRAGHAZ representation of a donor stack showing the stack axis and hazard volume (from NSWC TR 87-59).

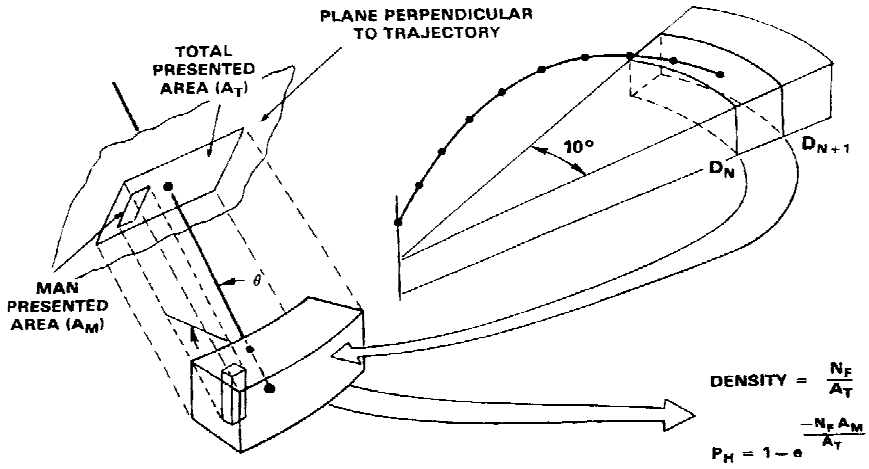

Figure 2. FRAGHAZ representation of target (acceptor) vulnerability and algorithm for determining hazard probability (from NSWC TR 87-59).

segment, various hit probabilities and fragment densities are accumulated and represented as functions of the downrange distance associated with the midpoint of the segment. A determination of whether or not the fragment is hazardous based on its kinetic energy is made. The hazard hit probabilities depend on the ratio of the presented area of the target to the presented area of the hazard-volume segment with respect to hazardous fragments as shown in Figure 2

FRAGPROP

While its basic features were retained, the modifications to FRAGHAZ were extensive. They proceeded in two phases: the first to streamline the existing code and the second to implement the required new models. The resulting code was renamed FRAGPROP. A flow chart applicable to both FRAGHAZ and FRAGPROP is shown in Figure 3.

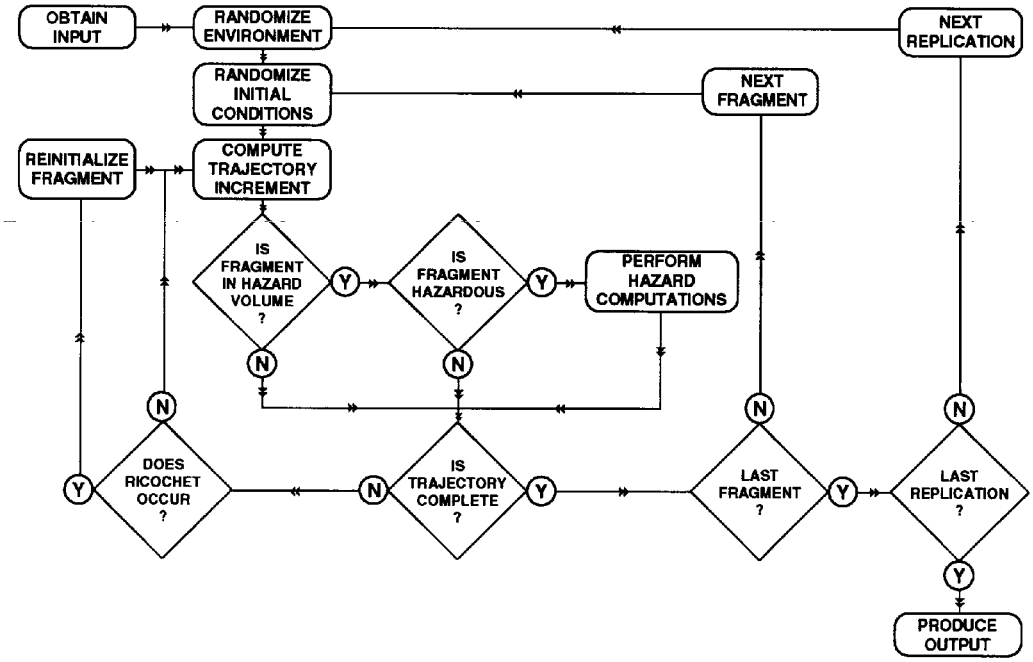

Figure 3. FRAGHAZ/FRAGPROP Flow Chart.

The original program made minimal use of modularization and was unwieldy to work with. We broke the code down into subroutines. As a result, the overall logic is easily followed in the main program. We changed the variable names to more descriptive forms that conform to FORTRAN naming conventions. In conjunction with this, we eliminated most of the type declarations. Many of the variables and computations were unnecessary for our purposes, and we eliminated them. Some expressions, although correct, were recast in order to eliminate mixed-type operations. Elseif constructions were eliminated for clarity, and less convoluted logic was substituted where possible. Execution speed was increased by moving expressions that had been repeatedly evaluated within loops to positions outside those loops and by eliminating redundant computations. For simplicity, we also eliminated the Full Factorial option.

New features and algorithms were also incorporated. Input was reorganized to read separate files for the run parameters, the donor description, and the acceptor description. Fragmentation data input was rewritten to reject

fragments not meeting user-specified criteria for minimum mass and initial elevation angle. The downrange segment size (which had been fixed at 100 ft) was generalized to accept user specification. Computation of vulnerable areas for the acceptor elements and algorithms for determination of the detonation, burn, and mechanical damage lethality of each fragment including the effects of container penetration were added. Finally, a determination and report of the minimum range at which the analysis is applicable were implemented. These algorithms are described in detail in the following sections.

DONOR MODELS

Stack Description. The donor stack is described as in the original FRAGHAZ code. The height of the bottom of the stack and the height of munitions in the stack are required to provide bounds for the initial height of each fragment. The size of the stack contributing to downrange fragmentation is described by specifying the number of "interaction areas" present on the downrange face of the stack. An interaction area is formed by each side-by-side pair of munitions. Thus, an arrangement of three projectiles in a row forms two interaction areas. If two such arrangements are stacked one on top of the other, four interaction areas result. However, if two such arrangements are set side by side (six rounds in a row), five interaction areas are produced. Interaction areas are considered instead of individual munitions because the effect of focusing along the plane of symmetry between the rounds augments the fragment velocities. Interaction areas are specified along with arena test data for multiple munitions. However, where data for single munitions (including estimated data) must be used, the donor unit is the single munition, and the number of munitions on the downrange face specifies the stack size.

Arena Test Fragmentation Data. Arena test data form the basis for describing the fragmentation characteristics of a particular munition. Data for interacting M107 projectiles including parameters for 215 fragments are provided with FRAGHAZ. Each fragment recovered in the test is characterized by five parameters: the polar zone of its origin, its mass, velocity, and area-to-mass ratio, as well as the ratio of its maximum to average presented area (to account for the effects of tumbling on aerodynamic drag).

Fragment multipliers (McClesky 1988) are used to normalize the data for scaling to any stack size (i.e., any number of interaction areas or munitions) and any hazard volume azimuthal sector width. One fragment multiplier must be supplied for each polar zone represented in the data. The formula for computing the fragment multiplier for the *i*th polar zone, ϕ_i, is

$$M_F(\phi_i) = \frac{1}{N_I \psi_s(\phi_i)} ,$$

where N_I is the number of interaction areas (or single munitions, if appropriate) in the face of the stack *from which the data were collected* and $\psi_S(\phi_i)$ is the azimuthal sector width over which fragments were collected in the ith polar zone.

Adapting Arena Test Fragmentation Data. Arena test data for single munitions tabulated in the Joint Munitions Effectiveness Manual of Fragmentation Data (FM 101-62-3) are not in the FRAGHAZ format and do not provide all of the parameters required. Data for individual fragments are not provided. Rather, the mean fragment weight and integrated number of fragments for 50-grain weight increments are tabulated along with the initial velocity for each polar zone. A shape factor, K (=0.5126 $cm^2/g^{2/3}$ for the M107), for all fragments is given and can be used in the expression

$$\frac{a_{f_{avg}}}{m_f} = \frac{K}{m_f^{1/3}} ,$$

to estimate the area to mass ratio of a fragment.

We expanded these data to generate a table of 870 individual fragments (as required by FRAGPROP) by rounding the integrated number of fragments for each polar zone and fragment mass increment to an integral value and generating table entries for that number of individual fragments. These fragments were each assigned the mean weight of the associated weight increment and the mean velocity of the associated polar zone. In doing this, it was possible to eliminate small fragments. Since the ratio of the fragments' maximum to average presented area is not given, we used the average value taken from the FRAGHAZ input data for M107 stacks:

$$\frac{a_{f_{max}}}{a_{f_{avg}}} = 1.479 .$$

For this arena test, there is only one unit in the stack, and the integrated number of fragments is adjusted to apply to the entire 360° azimuthal sector. Thus, the fragment multipliers are independent of polar zone ($M_F = 1/360 = 2.7778 \times 10^{-3}$).

A capability to invert the polar distribution of the donor fragmentation data was added to FRAGPROP in order to allow representation of a nose-down attacking projectile as the initial event in a propagation chain.

Estimating Fragmentation Data. The TOW-2A missile is not a fragmenting weapon, and fragmentation data are not available. We needed to estimate data having a representative distribution of values of the five parameters required by the FRAGPROP input. Several analytical techniques applicable to single cylindrical munitions are available for this purpose. The fragmentation unit in this case is a single munition rather than an interaction area. Thus, focusing effects are ignored, and the number of rounds is specified in lieu of the number of interaction areas. Geometric data required to represent the TOW-2A warhead and rocket motor as cylindrical components and energetic material performance data as needed for use with the following analyses are summarized in Appendix B.

The Mott equation (see Victor 1994) describes the distribution of fragment mass. The fraction, f, of fragments having a mass greater than m_f is given by

$$f(m_f) = \sqrt{\exp(-2m_f/\overline{m_f})} ,$$

where $\overline{m_f}$ is the average fragment mass. This equation may be solved for m_f.

$$m_f(f) = -\frac{1}{2}\overline{m_f}\ln(f^2) .$$

By selecting random values of f that are evenly distributed between 0 and 1, this equation may be used to generate sets of fragment masses having the Mott distribution. The total number of fragments is given by

$$n_f = \frac{m_c}{\overline{m_f}} ,$$

where m_c, the total mass of all fragments, may be identified with the casing mass. Victor also gives the average fragment mass as

$$\overline{m_f} = \frac{A}{p_d}\sqrt{1+\mu/2}\left[\frac{h_c}{d_x}\left(d_x+h_c\right)^{3/2}\right],$$

where A is a constant, p_d is the detonation pressure, μ is the ratio of the mass of the casing to the mass of the charge, h_c is the thickness of the casing, and d_x is the diameter of the explosive or propellant charge (equal to the inside diameter of the casing). A = 676.2 g-kbar/in$^{3/2}$ for mass in grams, pressure in kilobars and distance in inches. The Kamlet-Jacobs formula may be used to estimate the detonation pressure (in gigapascals) if it is not otherwise known.

$$p_d = 1.558\rho_o^2 N\sqrt{MQ},$$

where ρ_o is the unreacted density in grams per cubic centimeter, N is the number of moles of detonation product per gram of unreacted material, M is the average molecular weight of the detonation product gases, and Q is the chemical energy of the detonation reaction in calories per gram.

No method exists for predicting a distribution of fragment velocities. However, the Gurney equation (see Dehn 1984) may be used to estimate a single velocity for all fragments.

$$v_f = \frac{\sqrt{2E}}{\sqrt{\mu+1/2}},$$

where $\sqrt{2E}$ is a property of the energetic material (having the units of velocity) known as the Gurney constant. Its value may be found in the literature or estimated (in milliseconds) using the equation of Kamlet and Finger.

$$\sqrt{2E} = 233\frac{\sqrt{p_d}}{\rho_o^{0.6}},$$

for density in grams per cubic centimeter and detonation pressure in kilobars. Although this approach gives only one value of the fragment velocity, randomization over a narrow range takes place within FRAGPROP.

For estimating the area-to-mass ratio of a fragment, Victor (1994) gives the shape factor as K = 0.5199 cm^2/g$^{2/3}$ for randomly shaped fragments. We are not aware of any method to estimate the ratio of a fragment's maximum to average presented area, so we assumed a fixed value of 1.5.

The TOW-2A storage orientation is horizontal in contrast to that of the M107. Thus, it is necessary to interpret the (rather narrow) polar distribution of fragments with respect to the munition axis as an azimuthal distribution with respect to the stack axis. This is assumed to produce an azimuthal sector width of only 20°. Because the missile components are treated as horizontal cylinders, the polar distribution with respect to the stack axis is assumed uniform. Since the azimuthal sector width is independent of polar zone, the fragment multiplier is a constant (M_F = 1/20 = 0.05).

We wrote a short program (incorporating the FRAGHAZ random number generator) to produce FRAGPROP input data for a general warhead and rocket motor combination in accordance with the foregoing algorithms and

used it to generate data for 365 fragments from the TOW-2A warhead and flight motor. These components produce both aluminum and steel fragments. We neglected fragments from the launch motor, which has a small diameter.

ACCEPTOR MODELS

Stack Description. The basic acceptor stack description is given by providing dimensions of height (H_a), width (W_a), and depth (D_a). The storage orientation may be vertical, as with the M107, or horizontal, as with the TOW-2A. The vulnerable components of an acceptor may include a warhead, rocket motor, or both.

Vulnerable Areas. Vulnerable areas at the front and top of the stack are required. Side and back areas are excluded as the acceptor stack is assumed to face the donor. These depend on the ammunition dimensions and the storage orientation (horizontal or vertical).

For the purpose of determining hit probabilities the total front and top areas of the stack are considered vulnerable. The front vulnerable area is

$$A_{fh} = H_a W_a \ ,$$

and the top vulnerable area is

$$A_{th} = D_a W_a \ .$$

For mechanical damage, the vulnerable areas are the areas presented to the front and top faces of the stack of the entire weapon (represented as a cylinder of diameter D_w and length L_w) multiplied by the number of munitions in that face of the stack (N_f or N_t). The vulnerable areas depend on the storage orientation. For vertical storage, the front vulnerable area is

$$A_{fm} = N_f D_w L_w \ ,$$

and the top vulnerable area is

$$A_{tm} = N_t \pi \left(D_w/2\right)^2 \ .$$

For horizontal storage, the front vulnerable area is unchanged.

$$A_{fm} = N_f D_w L_w \ ,$$

while the top vulnerable area is

$$A_{tm} = N_t D_w L_w \ .$$

Similarly, for detonation and burning, the *maximum* vulnerable areas are those of the energetic materials in the warhead and/or rocket motor (cylinders of diameter D_x and length L_x) presented to the front and top faces of the stack. For vertical storage, the front maximum vulnerable area is

$$A_{fx_{max}} = N_f D_x L_x \ ,$$

and the top maximum vulnerable area is

$$A_{tx_{max}} = N_t \pi \left(D_x/2\right)^2 \ .$$

For horizontal storage, the front maximum vulnerable area is

$$A_{fx_{max}} = N_f D_x L_x \ ,$$

and the top maximum vulnerable area is

$$A_{tx_{max}} = N_t D_x L_x \ .$$

Here, the subscript x represents either the warhead explosive or rocket motor propellant.

With respect to a particular fragment, the vulnerable areas for detonation and burning may be further limited depending on the velocity and diameter of that fragment. Below some critical threshold, none of the presented area of an energetic component is vulnerable. Above the threshold, part or all of the areas is vulnerable. Partial vulnerability is generally a function of the maximum obliquity, θ_{max}, from the normal to the surface of the weapon component at which an impacting fragment can produce reaction. Expressions for θ_{max} for detonation and burning are developed in the following sections.

Detonation Vulnerability. The vulnerability of a weapon component to initiation of detonation by fragment impact is described by the Jacobs-Roslund formula (Liddiard and Roslund 1993) for critical impact velocity. This formula applies to cylindrical projectiles having diameters greater than the failure diameter of the energetic material.

$$v_{jr} = \frac{a_{jr}\left(1 + b_{jr}\right)\left(1 + c_{jr}\dfrac{h_c}{d_f}\right)}{\cos\theta\sqrt{d_f}} \ ,$$

where a_{jr}, b_{jr}, and c_{jr} are characteristic constants that have been determined for a number of explosives. Values of the Jacobs-Roslund constants used in conjunction with our analysis are given in Appendix B. It is assumed that the fragment always strikes the vulnerable component with an average value of presented area. Thus, the fragment diameter, d_f, may be determined from the average fragment presented areas assuming a circular cross section,

$$d_f = 2\sqrt{\frac{a_{f_{avg}}}{\pi}} \ .$$

The angle θ is the obliquity of the fragment with respect to the normal to the surface of the casing. The obliquity dependence of the critical velocity may be expressed as

$$v_{jr}(\theta) = \frac{v_{jr}(0)}{\cos\theta} \ .$$

We define the maximum obliquity that can produce detonation for a fragment with velocity, v_f, such that

$$v_{jr}(\theta_{max}) = v_f \ .$$

Thus,

$$\cos\theta_{max} = \frac{v_{jr}(0)}{v_f} ,$$

and θ_{max} is defined for $v_f \geq v_{jr}(0)$. This represents the critical condition. This model has been calibrated for steel fragments. However, we also used this calibration for the aluminum fragments produced by the TOW-2A warhead casing. As a worst case, we assumed that the fragments were flat-ended cylinders ($b_{jr} = 0$ with an appropriate value for c_{jr}) and that the critical diameter of the energetic material was always smaller than the diameter of the fragment. Since actual fragments rarely exhibit this morphology, a more realistic simulation might result from a random selection of the critical velocity between limits for flat- and round-ended cylindrical fragments.

Burning Vulnerability. The vulnerability of a weapon component to initiation of burning may be associated with perforation of the casing by the fragment. This is particularly true in the case of thin-walled munitions (Gilman). Some critical residual velocity, v_{rc}, may be required to produce reaction. The THOR velocity equation relates the residual velocity, v_r, to the initial velocity, v_f, for a penetrating fragment.

$$v_r = v_f - 10^{a_v} \left(h_c a_{f_{avg}}\right)^{b_v} m_f^{c_v} v_f^{d_v} / \left(\cos\theta\right)^{e_v} .$$

Again, it is assumed that the fragment strikes the vulnerable component with an average value of presented area. With $v_r = v_{rc}$ at $\theta = \theta_{max}$,

$$\cos\theta_{max} = \left[\frac{10^{a_v}\left(h_c a_{f_{avs}}\right)^{b_v} m_f^{c_v} v_f^{d_v}}{v_f - v_{rc}}\right]^{1/e_v} ,$$

and θ_{max} is defined for

$$v_f - v_{rc} \geq 10^{a_v}\left(h_c a_{f_{avg}}\right)^{b_v} m_f^{c_v} v_f^{d_v} .$$

This expression represents the critical condition. Values of the THOR constants used in conjunction with our analysis are given in Appendix B. Since appropriate values of the critical residual velocity are not known, we used $v_{rc} = 0$ as a worst case. This model has also been calibrated for steel fragments, but, again, we used the same calibration for the aluminum fragments produced by the TOW-2A warhead casing.

Comparison of Detonation and Burning Thresholds. It is tempting to presume that the less violent burning response is easier to produce than detonation. However, comparison of the critical velocities predicted by these models shows that this is not always the case. Critical velocities for detonation and burning of a typical fragment are plotted as functions of casing thickness in Figure 4. For thin, easily perforated casings (e.g., ~1 mm for the TOW-2A), burning is produced by fragments having much lower velocities than those required to produce detonation. (This result would still hold if a nonzero critical residual velocity of expected magnitude were used.) For thicker casings (e.g., ~15 mm for the M107), casing perforation is extremely difficult to achieve, but detonations may be produced at lower velocities due to the transmitted shock.

The point of intersection of the two threshold curves varies with the shape of the fragment (represented by the area-to-mass ratio). For ratios lower than the 10-in^2/lb value used in Figure 4, the point of intersection is

shifted toward high values of casing thickness. Thus, results are sensitive to assumptions regarding fragment orientation (presented area) at impact

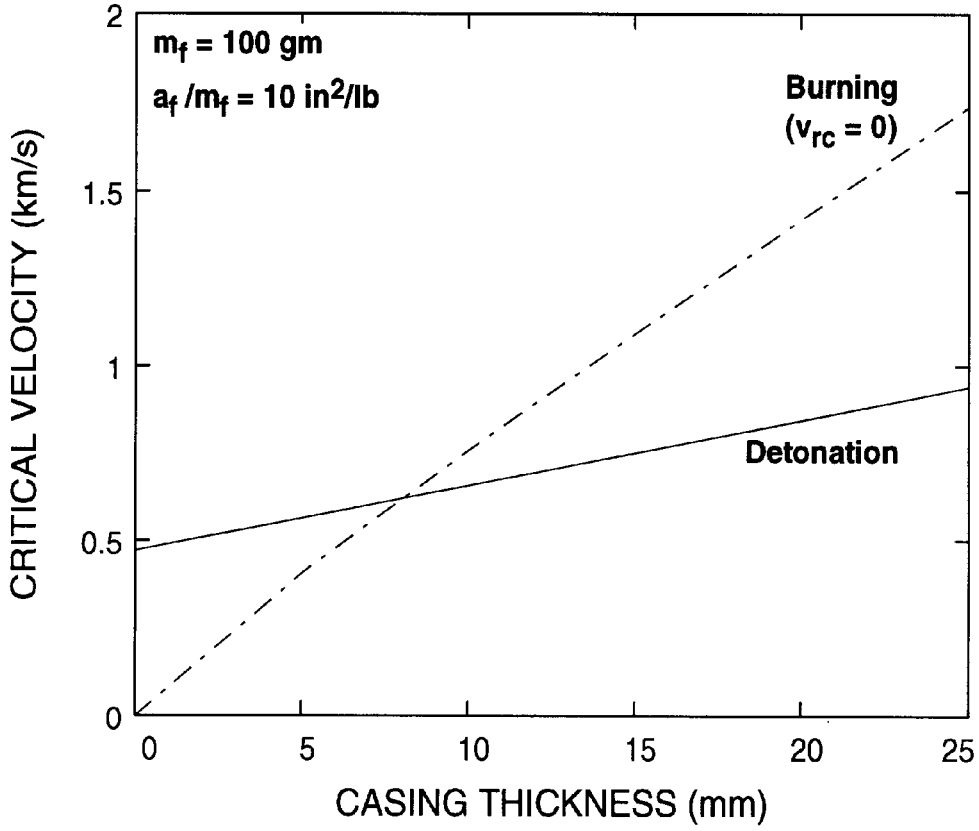

Figure 4. Comparison of critical velocities for detonation and burning.

Vulnerable Area Reduction. If the angle subtended at the center of the cylinder representing a vulnerable component by the region on the surface over which an impacting fragment is lethal with respect to detonation or burning ($\theta \leq \theta_{max}$) is $2\beta_{max}$ as shown in Figure 5, then the reduction in the maximum vulnerable area of that component is given by

$$A = \sin\beta_{max} A_{max} .$$

The relationship between θ_{max} and β_{max} depends on the storage orientation. For horizontal storage,

$$\beta_{max} = \theta_{max}$$

as shown in Figure 6. For vertical storage, the elevation angle of the fragment trajectory, α_f, must be accounted for, as shown in Figure 7. Thus,

$$\cos\beta_{max} = \frac{\cos\theta_{max}}{\cos\alpha_f} .$$

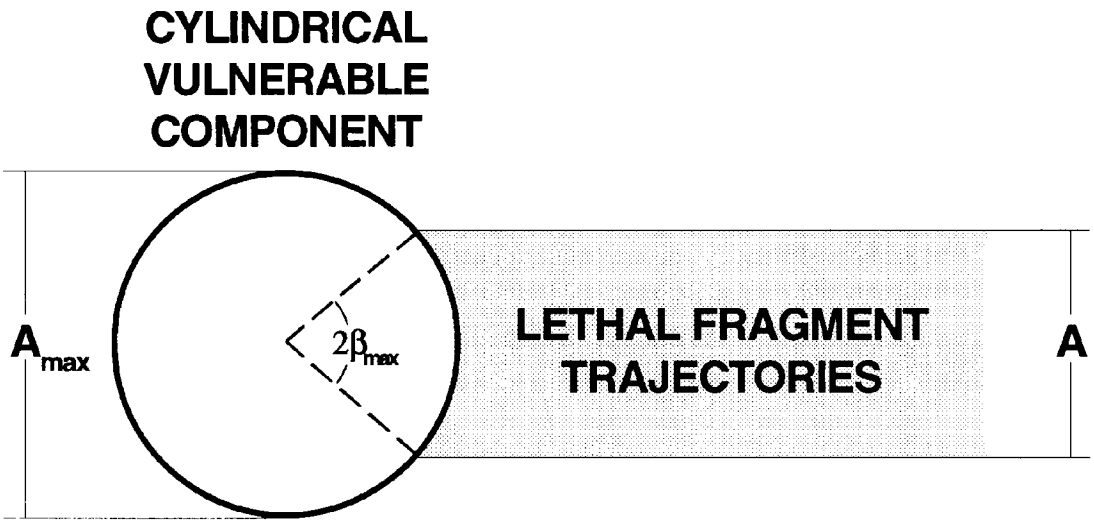

Figure 5. Angular region of vulnerability on a cylindrical charge.

Mechanical Damage Vulnerability. A single mechanical damage criterion based on kinetic energy applies to all weapon components. The stack is considered vulnerable to damage when the kinetic energy of a fragment exceeds a specified value, regardless of the obliquity. Accurate threshold values are not known, so we arbitrarily chose 400 and 50 ft-lb as the critical kinetic energy for the M107 and TOW-2A, respectively. The smaller value for the TOW-2A reflects its much thinner skin.

CONTAINER PENETRATION

The TOW-2A is packaged in a steel container, and provisions were made in FRAGPROP for estimating the reduction in fragment mass and velocity associated with penetration of the container. This occurs both when fragments are launched from a donor stack and when they impact an acceptor stack. In addition to the THOR velocity equation, the THOR mass equation is required.

$$m_r = m_f - 10^{a_m}\left(h_c a_{f_{avg}}\right)^{b_m} m_f^{c_m} v_f^{d_m} / (\cos\theta)^{e_m} .$$

Use of the THOR equations with $\theta = 0$ yields the maximum residual velocity and mass, representing the worst-case scenario. The residual diameter is determined from the residual mass, assuming that the area- to-mass ratio remains unchanged.

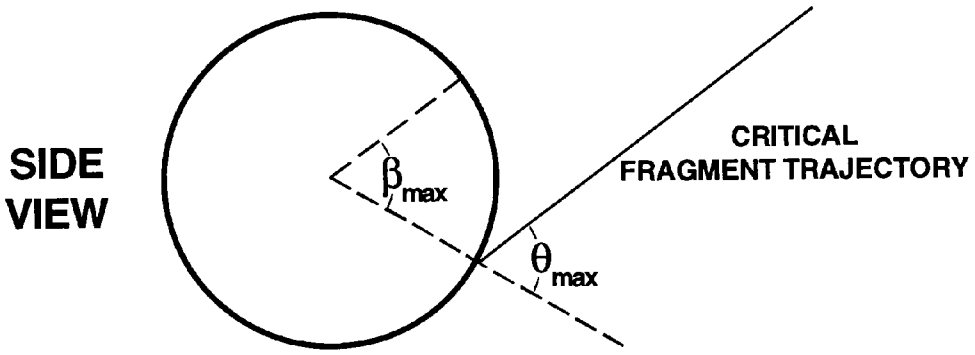

Figure 6. Relationship between the angular region of vulnerability and the maximum obliquity for horizontal storage.

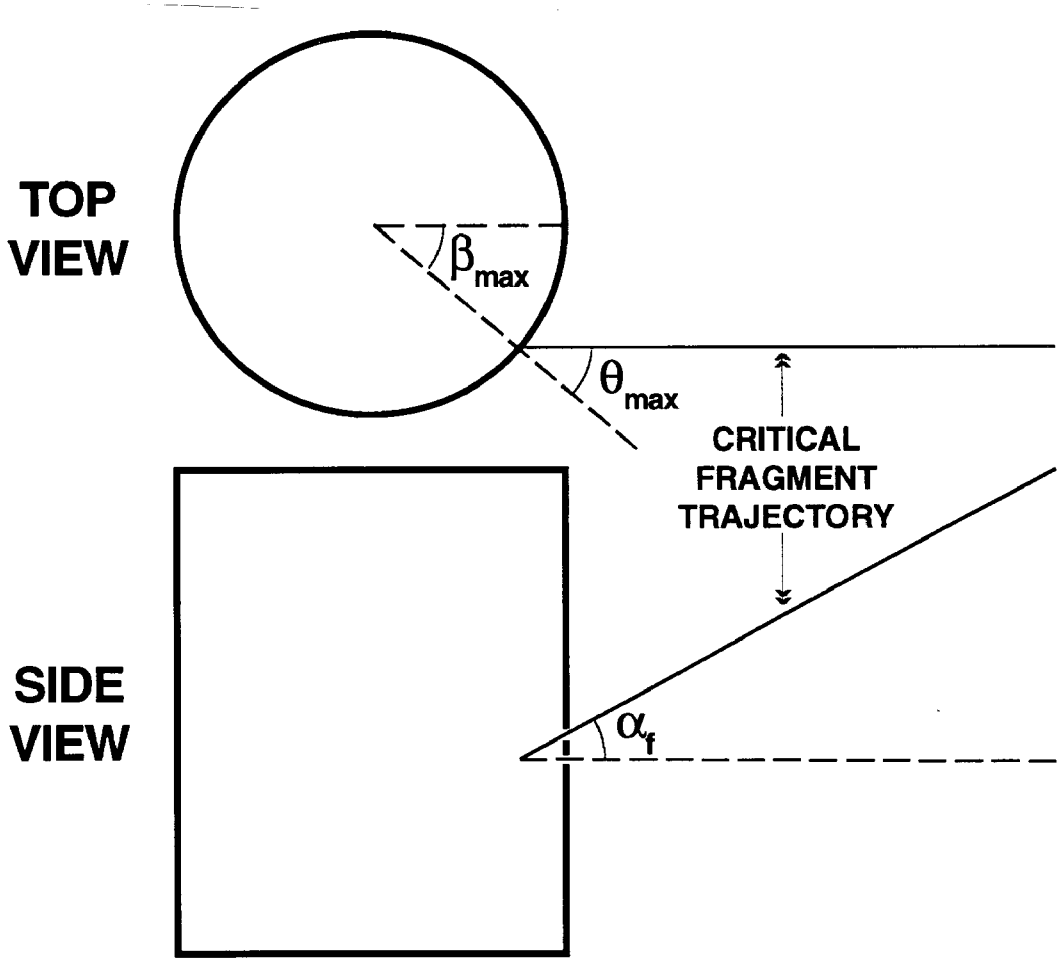

Figure 7. Relationship between the angular region of vulnerability, the maximum obliquity, and the fragment elevation angle for vertical storage.

MINIMUM RANGE

The FRAGHAZ analysis is applicable as long as the angle subtended by the acceptor stack does not exceed the width, ψ, of the azimuthal sector associated with the donor fragmentation data. The minimum range is thus given by

$$r_{min} = \frac{W_a}{2\tan(\psi/2)} .$$

Note that r_{min} is zero for sectors wider than 180°.

COMPUTATIONAL CONFIGURATIONS AND RESULTS

Theater of Operations Considerations. Storage regulations applicable to basic load ammunition holding areas in theaters of operations limit the explosive quantity in any stack to 4,000 kg (8,818 lb). Such stacks must be separated by at least 77 m (253 ft). (See Army Regulation 385-64.) We considered M107 and TOW-2A stacks containing approximately this maximum weight.

Each M107 projectile contains 15.4 lb of Composition B. Thus, a pallet of 8 projectiles contains 123.2 lb, and a stack of 72 pallets contains 8,870.4 lb.

A TOW-2A missile contains 6.7 lb of LX-14 plus 0.2 lb of other high explosives in the warhead, 1.2 lb of M7 propellant in the launch motor, and 7.0 lb of GCV propellant in the flight motor for a total of 15.1 lb. A pallet of 12 missiles contains 181.2 lb, and a stack of 48 pallets contains 8,697.6 lb.

Stack Arrangements. The arrangement of pallets affects the lethality and vulnerability of a stack. Consideration of the least and most lethal arrangements as well as the least and most vulnerable arrangements provides scope to a determination of propagation probabilities. Pertinent stack parameters may be estimated from pallet dimensions given in Appendix B.

Each M107 pallet contains eight vertical projectiles in an arrangement that is one projectile high, four projectiles wide, and two projectiles deep ($1 \times 4 \times 2$). The 72 pallets may be arranged in any permutation of $3 \times 4 \times 6$, where the first dimension is the height of the stack in pallets, the second dimension is the width of the stack in pallets, and the third dimension is the depth of the stack in pallets. Individual pallets retain their 1×4 x 2 orientations for all permutations. Table 1 gives the number of interaction areas, stack dimensions, and total front and top vulnerable area associated with each permutation.

The $4 \times 3 \times 6$ pallet arrangement is both least lethal (having the fewest interaction areas) and least vulnerable (having the smallest vulnerable area), while the $4 \times 6 \times 3$ arrangement is both most lethal and most vulnerable.

Table 1. Lethality and Vulnerability Parameters for M107 Stacks

Pallet Arrangement ($n_h \times n_w \times n_d$)	Number of Interaction Areas on Face of Stack	Stack Dimensions			Vulnerable Areas (front + top) (ft^2)
		height (ft)	width (ft)	depth (ft)	
3 × 4 × 6	45	8.00	9.63	7.20	146.3
3 × 6 × 4	69	8.00	14.50	4.77	185.2
4 × 3 × 6	44	10.67	7.20	7.20	128.6
4 × 6 × 3	92	10.67	14.50	3.55	206.2
6 × 3 × 4	66	16.00	7.20	4.77	149.5
6 × 4 × 3	90	16.00	9.63	3.55	188.3

Each TOW-2A pallet contains 12 horizontal missiles in an arrangement that is 3 missiles high, 1 missile wide, and 4 missiles deep (3 × 1 × 4). The 48 pallets may be arranged in any permutation of 3 × 4 × 4. Table 2 gives the number of missiles on the front face, stack dimensions, and total front and top vulnerable areas associated with each permutation.

Table 2. Lethality and Vulnerability Parameters for TOW-2A Stacks

Pallet Arrangement ($n_h \times n_w \times n_d$)	Number of Missiles on Face of Stack	Stack Dimensions			Vulnerable Areas (front + top) (ft^2)
		height (ft)	width (ft)	depth (ft)	
3 × 4 × 4	36	10.06	20.25	14.64	500.0
4 × 3 × 4	36	13.41	15.17	14.64	425.3
4 × 4 × 3	48	13.41	20.25	10.96	493.4

Based on the number of missiles on the front face, the 4 × 4 × 3 pallet arrangement is most lethal. The other two arrangements are nominally equal in lethality. The 3 × 4 × 4 arrangement is most vulnerable, while the 4 × 3 × 4 arrangement is least vulnerable. The missile stacks are considerably larger and more vulnerable to being hit than the artillery projectile stacks.

The single M107 projectile donor may be erect or inverted and may detonate at any specified height above the ground. The arrangements producing the least and greatest lethality are not apparent. However, preliminary computations indicated that the inverted round at the surface may be considered least lethal and the erect round at a 50-ft elevation most lethal.

Propagation Probabilities and Distances. The graphics program developed in conjunction with FRAGPROP plots the probabilities of exceeding the criteria for propagation of detonation (labeled D), burning (B), and mechanical damage (M), as well as the overall (lethal and nonlethal) hit probability (H) on a logarithmic scale as a function of range. A typical example is shown in Figure 8. The dashed vertical line near the probability axis indicates the minimum range for which the analysis is accurate.

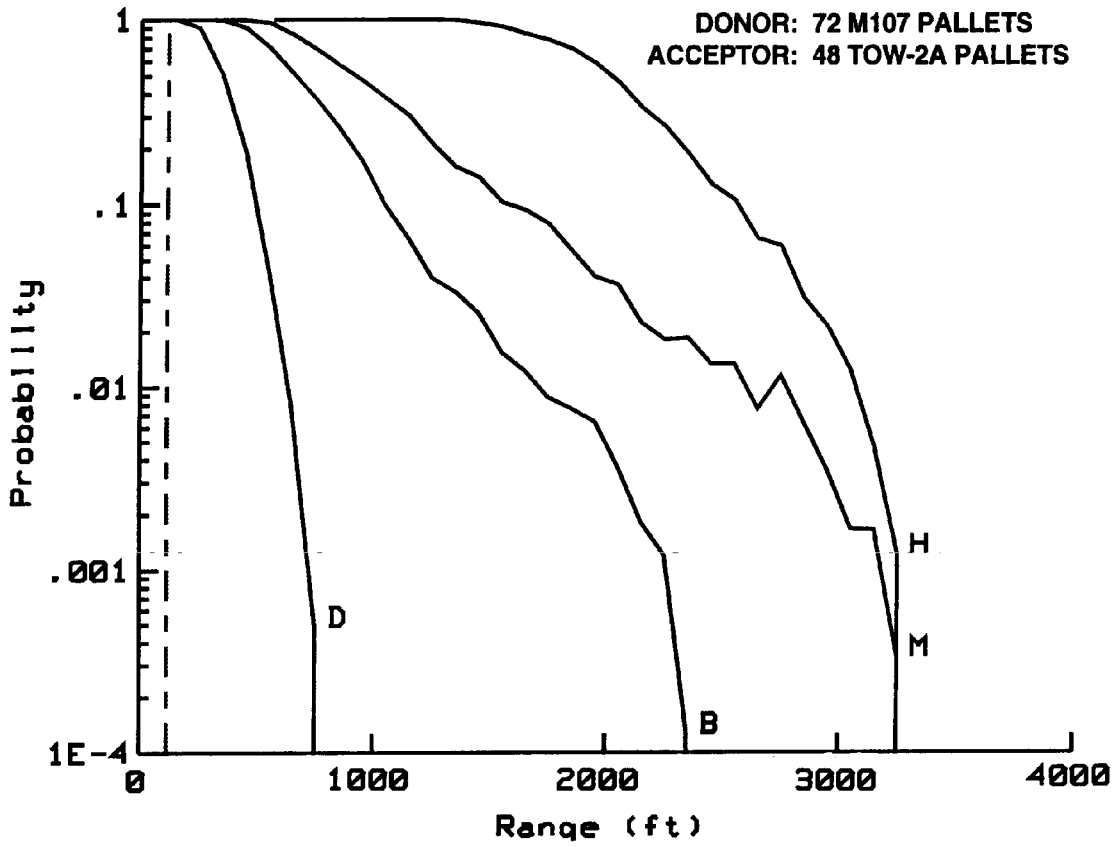

Figure 8. Probabilities of detonation, burning, mechanical damage, and hit as functions of range for an M107 donor stack against a TOW-2A acceptor stack.

Generally, the probabilities decrease with increasing range, and, theoretically, they can be expected to vanish entirely beyond some maximum range. For comparison purposes, it is often useful to consider the range at which a probability drops to some small value (e.g., 1%). The small probabilities predicted at long range may become nonmonotonic prior to vanishing. The ability to predict nonzero probabilities at long range is limited by the number of fragments in the donor data and the number of replications. Generally, the results are not accurate near vanishing probability. The number of replications required to produce monotonically decreasing probabilities varies inversely with the number of fragments describing the donor.

We made FRAGPROP computations using zero-wind conditions and soil constants varying between 0.5 and 4.0 for each of the three donors (single M107 projectiles, stacked M107 pallets, and stacked TOW-2A pallets) vs. both of the acceptors (stacked M107 and TOW-2A pallets). Preliminary computations were made to determine the maximum range required in each problem. Input conditions for the final computations are summarized in Table 3. These values depend on the donor and apply to both acceptors.

Table 3. FRAGPROP Computation Input Conditions

Donor	Number of Fragments	Number of Replications	Segment Size (ft)	Maximum Range (ft)
Single M107	870	50	50	2,400
M107 Stack	215	200	100	3,600
TOW-2A Stack	365	125	20	720

In order to determine the scope of probability values, two computations were made for each donor-acceptor pair: one for the least lethal donor stack arrangement against the least vulnerable acceptor stack arrangement and one for the most lethal donor stack arrangement against the most vulnerable acceptor stack arrangement. The graphics capability allows the four probabilities to be plotted as functions of range for two problems at a time as shown in Figures 9–14. Associated pairs of probability curves are joined by shading lines.

Results for single M107 donors against palletized M107 acceptors are shown in Figure 9. The probabilities decrease gradually with range. The distance at which the detonation propagation probability drops to 1% (on the upper curve of the pair) is 125 ft, while the 1% distance for burning is only 113 ft. Thus, burning propagation appears unlikely in this configuration. The probability of mechanical damage remains above 1% to a range of 687 ft, while the hit probability drops to 1% at 1,369 ft.

Similar results for single M107 donors against palletized TOW-2A acceptors are shown in Figure 10. The 1% distance for detonation is 162 ft, while a burn probability greater than 1% persists to a distance of 471 ft. The probability of mechanical damage drops to 1% at 666 ft. The range over which the overall hit probability remains above 1% is 1,551 ft.

Results for palletized M107 donors against palletized M107 acceptors are shown in Figure 11. Probabilities near unity persist to a greater range. This arrangement produces a 1% probability of detonation at 642 ft, while burning reactions propagate with a probability of 1% or greater over distances to 685 ft. The probability of mechanical damage remains above 1% to 2,871 ft. The 1% distance for the overall hit probability is 2,950 ft.

Similar results for palletized M107 donors against palletized TOW-2A acceptors are shown in Figure 12. This arrangement produces a 1% probability of detonation at 643 ft, while burning reactions propagate with a probability of 1% or greater over distances to 1,715 ft. A probability of mechanical damage greater than 1% persists to 2,779 ft. The 1% distance for the overall hit probability is 3,080 ft.

Results for palletized TOW-2A donors against palletized M107 acceptors are shown in Figure 13. Neither detonation nor burning propagation is predicted. The other probabilities remain high and then drop rapidly to zero with increasing range. Probabilities of mechanical damage exceeding 1% persist to 127 ft. The 1% distance for hit probability is 662 ft.

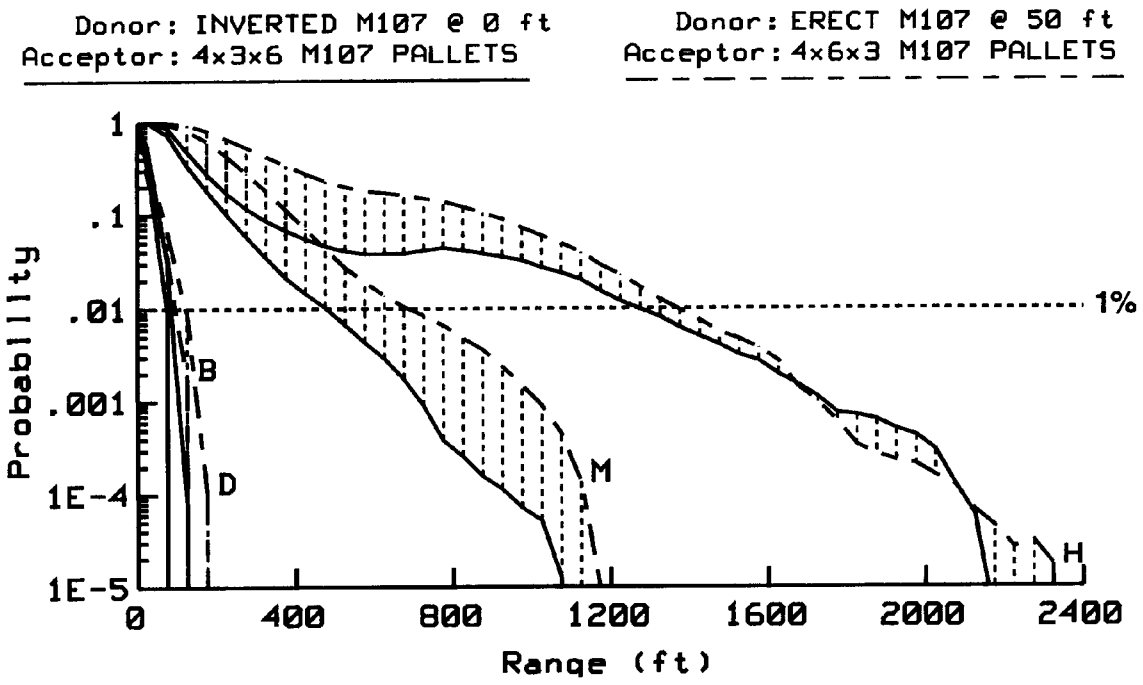

Figure 9. Probabilities of detonation, burning, mechanical damage, and hit as functions of range for single M107 donor projectiles against M107 acceptor stacks.

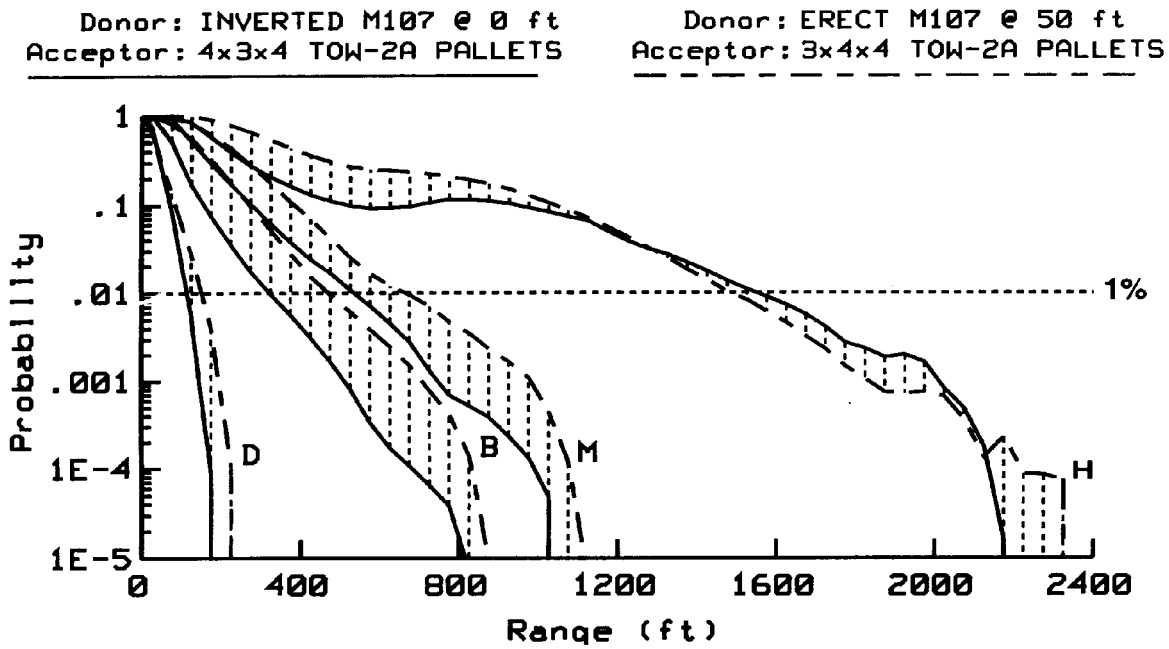

Figure 10. Probabilities of detonation, burning, mechanical damage, and hit as functions of range for single M107 donor projectiles against TOW-2A acceptor stacks.

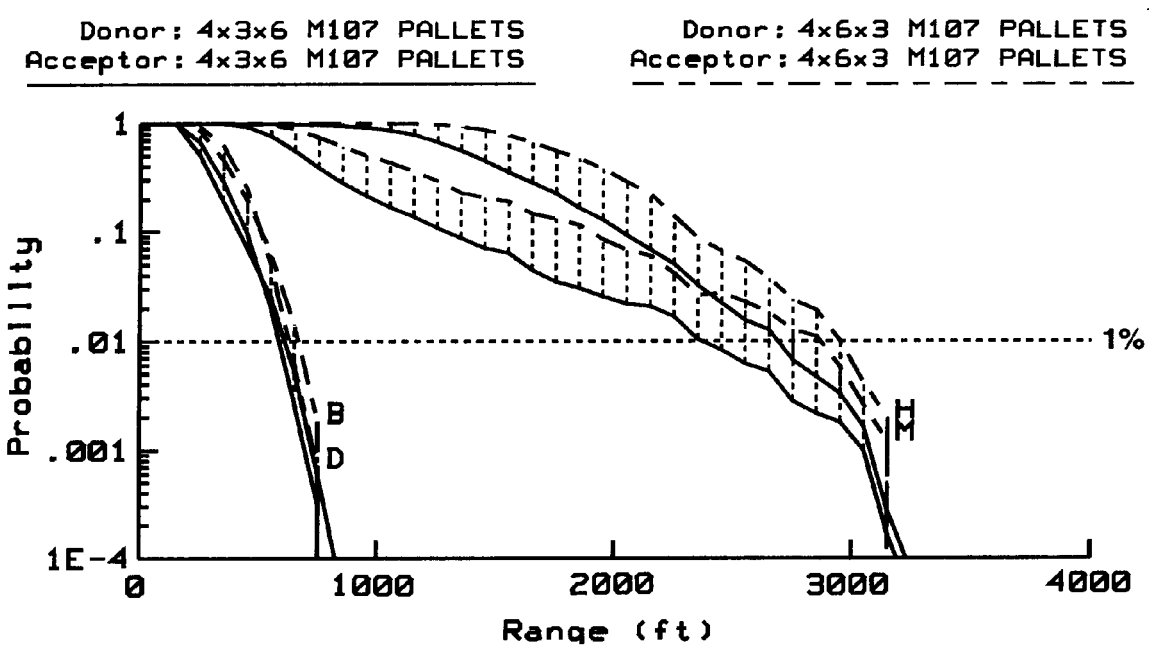

Figure 11. Probabilities of detonation, burning, mechanical damage, and hit as functions of range for M107 donor stacks against M107 acceptor stacks.

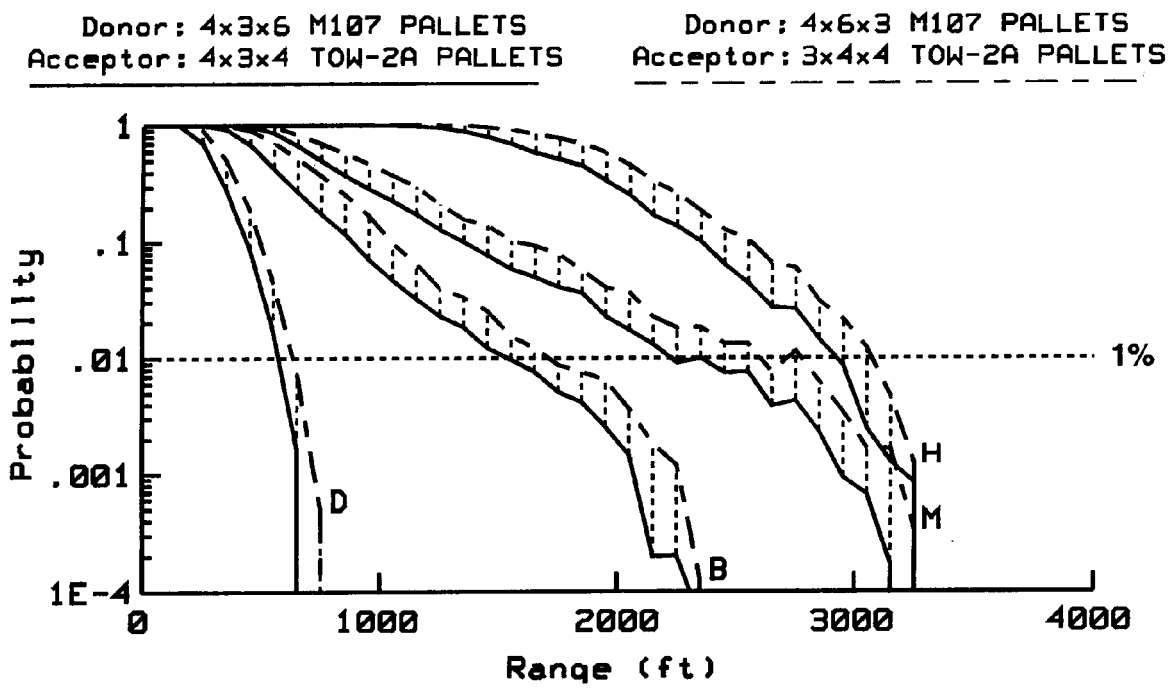

Figure 12. Probabilities of detonation, burning, mechanical damage, and hit as functions of range for M107 donor stacks against TOW-2A acceptor stacks.

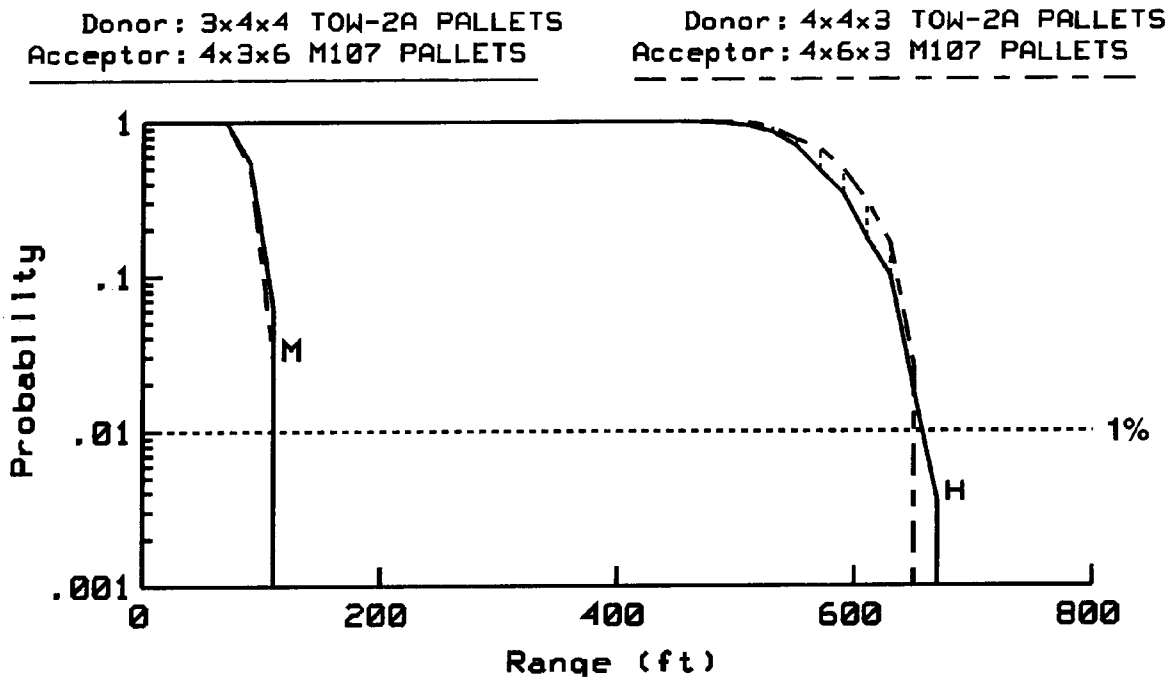

Figure 13. Probabilities of mechanical damage and hit as functions of range for TOW-2A donor stacks against M107 acceptor stacks.

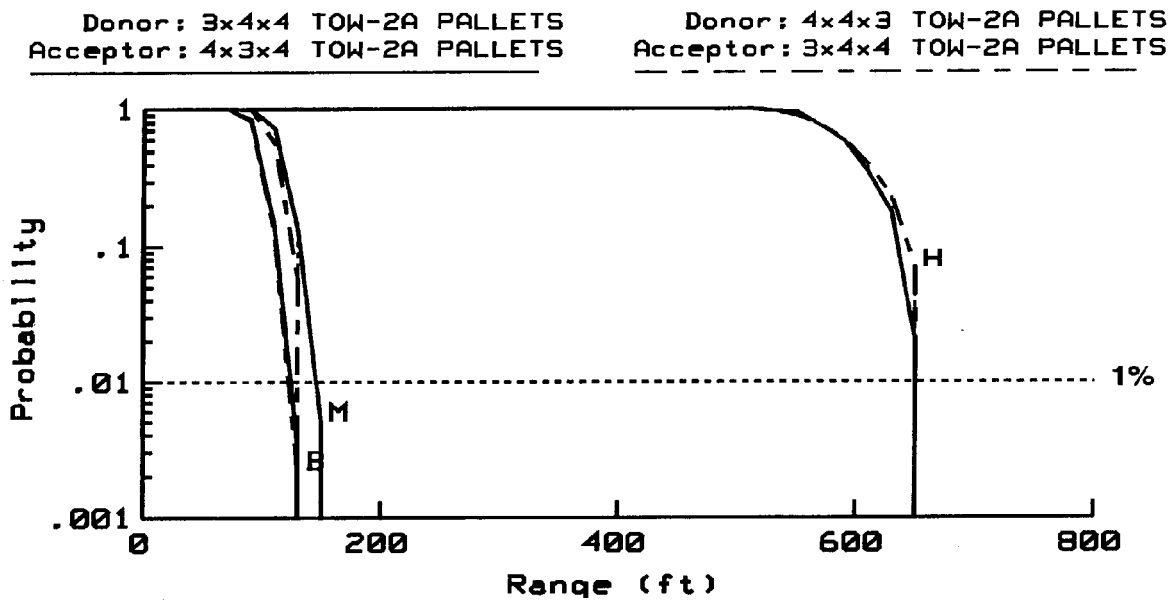

Figure 14. Probabilities of burning, mechanical damage, and hit as functions of range for TOW-2A donor stacks against TOW-2A acceptor stacks.

Similar results for palletized TOW-2A donors against palletized TOW-2A acceptors are shown in Figure 14. No detonation propagation is predicted, but burning propagation occurs at the 1% probability level out to a range of 129 ft. Probabilities of mechanical damage of 1% or greater persist to 149 ft. The 1% distance for hit probability is 667 ft. The fact that the burn and mechanical damage curves nearly coincide indicates that the arbitrary kinetic energy threshold for mechanical damage is too high.

The 1% propagation probability ranges discussed in the foregoing paragraphs are summarized in Table 4.

The lethality of the three donors varies substantially. Significant differences between the single and palletized M107 donors occur simply because of the number of munitions involved. The probabilities for these donors drop slowly, and the maximum ranges are considerably greater than the 1% ranges. TOW-2A donors are much less lethal due to the small fragments they produce. The character of the probability curves for these donors is different. Probabilities remain high until approaching the maximum range where they drop sharply.

Table 4. 1% Propagation Probability Distances (ft)

Donor	Acceptor	Detonation	Burning	Mechanical Damage	Hit
Single M107	M107 Stack	124	113	687	1,369
	TOW-2A Stack	162	471	666	1,551
M107 Stack	M107 Stack	642	685	2,871	2,950
	TOW-2A Stack	643	1,715	2,779	3,080
TOW-2A Stack	M107 Stack	No Prop	No Prop	127	662
	TOW-2A Stack	No Prop	129	149	667

The relative vulnerability of the two acceptors depends on the type of response. The TOW-2A is considerably more susceptible to burning than the M107. For the other responses, the 1% propagation distances are generally very similar. Although the (rather arbitrary) kinetic energy threshold is lower for TOW-2A acceptors, their probability of mechanical damage is reduced due to the presence of the container.

It is notable that this analysis (which includes a number of worst-case assumptions) does not preclude propagation of detonation from M107 stacks stored at the required 253-ft distance from either acceptor. At 250 ft, the probability of detonation propagation to an M107 stack is between 68% and 94% (depending on the stack configurations), and the probability of detonation propagation to a TOW-2A stack is between 71% and 91%.

SUMMARY AND CONCLUSIONS

By combining several existing models, we have developed a tool (FRAGPROP) for estimating the probabilities associated with the propagation of reaction between user-described ammunition stacks. The acceptor responses considered include detonation of energetic materials, burning of energetic materials (but not of combustible packaging), and mechanical damage. The models include the FRAGHAZ program for the Monte Carlo treatment of fragment trajectories and the accumulation of hit probabilities, the Jacobs-Roslund criterion for initiation of detonation, and the ballistic limit condition for initiation of burning.

A number of difficulties arose in applying this tool to munitions of interest. Since the appropriate fragmentation input data were not always available, notably in the case of missiles, we developed methods of estimating these data. It was necessary to represent the vulnerability of explosives and propellants for which Jacobs-Roslund parameters are not available using estimates based on values for similar compositions. It was also necessary to assess the lethality of aluminum fragments with models intended for use with steel fragments.

Although only two weapons have been specifically analyzed, the responses of the thick-walled M107 and the thin-walled TOW-2A are expected to encompass the range of responses of a wide variety of munitions. The analysis was used to predict distances below which the propagation probabilities for each response exceed 1% (see Table 4). Based on these predictions, we conclude that the artillery ammunition donor stacks are much more lethal than the missile donor stacks (which cannot produce detonation) and the missile acceptor stacks are more vulnerable to the propagation of burning (but not of detonation) than the artillery ammunition acceptor stacks. However, different assumptions regarding the orientation of fragments at impact time might enhance sensitivity to burning.

REFERENCES

Dehn, J. T. "Models of Explosively Driven Metal." BRL-TR-2626, U.S. Army Ballistic Research Laboratory, Aberdeen Proving Ground, MD, December 1984.

Department of the Army. "Ammunition and Explosives Safety Standards." AR 385-64, 22 May 1987.

Department of the Army. "Joint Munitions Effectiveness Manual of Fragmentation Data." FM 101-62-3.

Gilman, R. D. "Cased Granular Propellant Ignition." Date and source unknown.

Liddiard, T. P., and L. A. Roslund. "Projectile/Fragment Impact Sensitivity of Explosives." NSWC TR 89-184, Naval Surface Warfare Center, Silver Spring, MD, June 1993.

McClesky, F. "Quantity-Distance Fragment Hazard Computer Program (FRAGHAZ)." NSWC TR 87-59, Naval Surface Warfare Center, Silver Spring, MD, February 1988.

Victor, A. C. "Prediction/Analysis of Munition Reactions for Insensitive Munitions Threat Hazard Assessment." Proceedings of the Insensitive Munition Technology Symposium, Williamsburg, VA, June 1994.

APPENDIX A:

PROPAGATION ACCIDENTS IN AMMUNITION HOLDING AREAS

We considered several sources of information that are pertinent to propagation accidents in ammunition holding areas. These include reports of actual events found in the files of the Department of Defense Explosive Safety Board as well as results of hazard classification, packaging, and MILVAN tests.

At least 57 accidents involving open storage of ammunition have been identified. We have reviewed reports of many of these. There are a number of difficulties associated with the data given in these reports. Much of it is old, dating to the World War II era. The observations were made at different times by different people with different ideas about what is important. The amount of information reported varies widely, and details of storage configurations were not usually included.

We drew a number of conclusions from our review. En masse detonation of large quantities of ammunition is rare, usually involving bombs or large projectiles. More commonly, propagation accidents follow a sequence of events involving fire in an ammunition stack and cookoff of munitions in that stack. This leads to propagation of fire to neighboring stacks via hot fragments and burning debris. The process is then repeated in events which may take days to unfold. Propulsive reactions in which items such as rockets and mortar rounds are launched toward neighboring or distant stacks often contribute to propagation. White phosphorus rounds are also major contributors to this type of propagation. Three illustrative accident reports are summarized in Table A-1.

The most relevant hazard classification test is the bonfire test. While this provides the maximum fragment radius, it doesn't always identify the number of fragments that travel shorter distances. Distances over which firebrands are spread are usually not reported. Another relevant series of tests was conducted in MILVAN containers.[1] Although the quantities of explosive in each MILVAN were modest, items were thrown large distances.

The importance of packaging was demonstrated by Teitell and Reeves,[2] who conducted tests to determine the vulnerability of several munitions in wood packaging to several threats. The general results of these tests were that the threats did not cause detonations but started fires in propellants and wood packaging. Propellant fires rapidly cooked off warheads, and wood fires cooked off warheads, causing both detonations and less violent explosions. Detonations sometimes scattered stacks and stopped reaction. Fire-resistant packaging prevented the spread of reaction in some cases.

We conclude that the dominant mode of propagation in ammunition accidents is fire leading to cookoff leading to more fire and more cookoff. Combustible packaging and propulsive reactions are major contributors to propagation. Insensitive munition technology will reduce the probability of propagation, especially where stacks can be separated by more that 50 ft. However, quantitative analysis of propagation probability for this mechanism is probably not possible at this time.

---

[1] Lawrence, W. "Fragment Hazards From Munitions in Containers." BRL-TR-3203, U.S. Army Ballistic Research Laboratory, Aberdeen Proving Ground, MD, 1991.

[2] Teitell, L., and H. J. Reeves. "Fire Retardant Packaging for Artillery Ammunition." BRL-MR-2490, U.S. Army Ballistic Research Laboratory, Aberdeen Proving Ground, MD, 1975.

Table A-1. Summary of Representative Propagation Accident Reports

DDESB File	466	480	1271
Location	Pueblo, CO	Ie Shima, Japan	Da Nang, Vietnam
Ammunition	3 "Piles" of TNT-Loaded 3-in M42 Ammunition Separated by 120 ft and 285 ft	2,162 Tons of Bombs, Rockets, Small Arms, 20 mm in Open Storage With About 200 ft Between Stacks	Large Marine Corps Ammunition Supply Point
Cause	Lightning		Fire, Possibly Caused by Enemy Action
Duration	Hours	2 Days	>24 Hours
Result	●Multiple Events ●Fire Spread by Hot Fragments and Burning Debris ●Virtually All Ammo Lost ●Frags to 3,700 ft ●Thrown Round Detonated on Impact at 200 ft ●Burning Wood and Fiberboard Traveled 400 ft	Essentially Everything Lost	●Multiple Explosions ●Rockets Communicated Reaction to an Air Force ASP ●Large Loss of Ammo ●"No Cell Appeared to Communicate Directly to Its Neighbor"

APPENDIX B:

LETHALITY AND VULNERABILITY DATA

The data required for M107 and TOW-2A lethality and vulnerability descriptions are summarized in Tables B-1 through B-5.

Table B-1. Weapon Dimensions and Materials

Component	M107	TOW-2A
Weapon:		
Outside Diameter	6.10 in	6.187 in
Length	23.90 in	60.000 in*
Warhead:		
Outside Diameter	6.10 in	5.850 in
Length	23.90 in	25.570 in
Casing Material	steel	aluminum
Casing Thickness	0.63 in	0.050 in
Explosive Type	Comp. B	LX-14
Charge Diameter	4.84 in	5.750 in
Charge Length	20.30 in	9.574 in
Rocket Motor:		
Outside Diameter	N/A	5.837 in
Length	N/A	18.700 in
Casing Material	N/A	steel
Casing Thickness	N/A	0.055 in
Propellant Type	N/A	GCV
Charge Diameter	N/A	5.782 in
Charge Length	N/A	6.320 in
Container:		
Material	N/A	steel
Outside Diameter	N/A	10.000 in
Thickness	N/A	0.040 in
Pallet:		
Orientation	vertical	horizontal
Arrangement (H × W × D)	1 × 4 × 2	3 × 1 × 4
Weapon Spacing	1.20 in	1.000 in*
Elevation	8.10 in	8.100 in*
Height (with pallet)	32.00 in	40.220 in
Width	28.00 in	60.000 in
Depth	13.40 in	43.160 in

* estimated value

Table B-2. Energetic Material Performance Parameters

Material	Density (g/cm^2)	Detonation Pressure (kbar)	Gurney Constant (m/s)	Product Gases (mole/g)	Molecular Weight	Heat of Detonation (cal/g)
LX-14	1.83	370.0	2,948.0	Not Required	Not Required	Not Required
GCV Propellant	1.8	Unavailable	Unavailable	0.042156	24.635	890.0

Table B-3. Jacobs-Roslund Constants

Material	a_{jr} $\left(mm^{3/2}/\mu s\right)$	b_{jr}	c_{jr}
Composition B	3.065	0.0	1.70
LX-14*	3.6	0.0	1.59
GCV Propellant*	4.8	0.0	1.3

* estimated values

Table B-4. THOR Velocity Equation Constants

Material	a_v	b_v	c_v	d_v	e_v
mild steel	3.6901	0.889	−0.945	0.019	1.262
aluminum	3.9356	1.029	−1.072	−0.139	1.251

Table B-5. THOR Mass Equation Constants

Material	a_m	b_m	c_m	d_m
mild steel	−2.478	0.138	0.835	0.761